

# Recent Development of Chemigenetic Hybrid Voltage Indicators Enabled by Bioconjugation Chemistry

Shuzhang Liu and Peng Zou\*



Cite This: *Bioconjugate Chem.* 2024, 35, 1711–1715



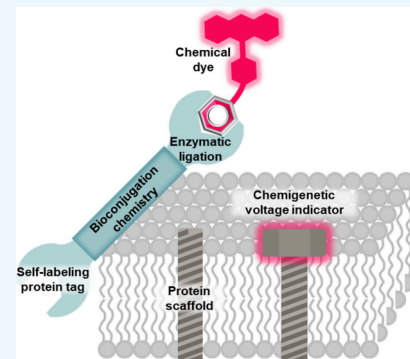
Read Online

ACCESS |

Metrics & More

Article Recommendations

**ABSTRACT:** Fluorescent voltage indicators enable the optical recording of electrophysiology across large cell populations with subcellular resolution; however, their application is often constrained by a limited photon budget. To address this limitation, advanced bioconjugation methods have been employed to site-specifically attach bright and photostable organic dyes to cell-specific protein scaffolds in live cells. The resulting chemigenetic hybrid voltage indicators enable sustained monitoring of voltage fluctuations with an exceptional signal-to-noise ratio, both *in vitro* and *in vivo*. This Viewpoint discusses recent advancements in the development of these indicators through bioconjugation chemistry.



## INTRODUCTION

Membrane potential controls many fundamental aspects of cellular physiology, including ion flux, vesicular release, and receptor signaling.<sup>1</sup> In excitable cells, such as neurons, cardiomyocytes, and pancreatic islet cells, rapid changes in the membrane potential form action potential (AP) spikes that are closely linked to brain cognition, cardiac pacing, and hormone secretion, respectively.<sup>2–4</sup> Compared to traditional micro-electrode-based approaches, genetically encoded voltage indicators (GEVIs) enable noninvasive recording of electrical signals in specific cell types with single-cell resolution across a large cell population. GEVIs operate through the mechanisms of either electrochromism or voltage-driven conformational changes. Electrochromic voltage sensing is exemplified by rhodopsin-based indicators, which exhibits voltage-dependent changes in optical absorption. Alternatively, engineered membrane proteins containing a voltage-sensing domain (VSD) could change their conformations in response to changes in membrane voltage. In both cases, voltage signal modulates the fluorescence emission of an appended fluorescent protein. However, the poor brightness and/or low photostability of fluorescent protein-based voltage indicators, particularly those in the far-red channel (emission wavelength > 650 nm), has made it difficult to meet the high photon budget demand required for high-speed, long-term voltage imaging.<sup>5,6</sup>

By leveraging the high specificity and efficiency of bioconjugation chemical reactions, a palette of bright and photostable organic dyes can be ligated to voltage-sensing protein scaffolds in live cells, replacing fluorescent proteins as the reporter. Two major approaches to protein labeling have

been employed to achieve this goal. The first one is the probe incorporation mediated by enzymes (PRIME), which uses an engineered bacterial lipoate protein ligase (LplA) to site-specifically conjugate a small molecule to a 13-amino acid LplA acceptor peptide (LAP).<sup>7,8</sup> The second one involves using a self-labeling protein tag, such as HaloTag. HaloTag is an engineered catalytically dead enzyme mutant that specifically recognizes and binds to its cognate suicidal substrates.<sup>9,10</sup> Chemigenetic hybrid voltage indicators, resulting from the above two approaches, have exhibited improved brightness and/or photostability in voltage sensing applications.<sup>11,12</sup> In this Viewpoint, we summarize the applications of bioconjugation approaches in developing chemigenetic hybrid voltage indicators.

## BIOCONJUGATION VIA ENZYME-MEDIATED PROBE INCORPORATION

The microbial rhodopsin Ace2 has been engineered for developing chemigenetic hybrid voltage indicators. As a photosensitive proton pump from *Acetabularia Acetabulum*, Ace2 contains a retinal chromophore covalently linked via a Schiff base. Mutations introduced in the path of proton transport block the photocurrent of Ace2 and alter the protonation state of the retinal Schiff base.<sup>13–15</sup> In several mutants, changes in

Received: August 27, 2024

Accepted: October 17, 2024

Published: October 30, 2024



ACS Publications

© 2024 American Chemical Society

membrane potential induce reversible alterations in the protonation level of the Schiff base, which in turn affect the absorption spectrum of Ace2, resulting in electrochromism.<sup>16</sup> If a fluorescent donor, such as a fluorescent protein, is linked to Ace2, changes in the rhodopsin absorption could alter the emission efficiency of the donor via Förster resonance energy transfer (FRET). Hence, voltage signals can be detected by monitoring the fluorescence intensity of the donor fluorophore (Figure 1).<sup>16,17</sup>

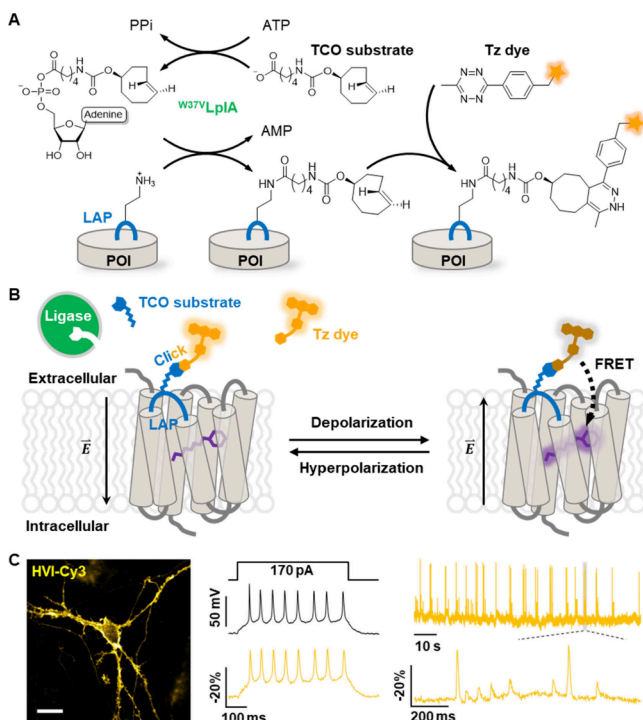


**Figure 1.** Chemigenetic voltage indicators enabled by enzyme-mediated probe incorporation. (A) Scheme of enzyme-mediated probe incorporation. Step one: enzymatic ligation of trans-cyclooctene (TCO) substrate to the LAP peptide; step two: TCO reacts with tetrazine (Tz)-conjugated dye via inverse electron demand Diels–Alder reaction (IEDDA). (B) Scheme of fluorescence labeling and the electrochromic FRET voltage sensing mechanism of HVI. (C) Representative confocal image of a cultured rat hippocampal neuron labeled with HVI-Cy3 (left, scale bar = 20  $\mu$ m), simultaneous electrical recording (black trace) and HVI-Cy3 imaging (orange trace) of an AP spike train (middle), and the recording of spontaneous voltage activities from a neuron (right), with a zoom-in view of the shaded region shown at the bottom.<sup>6</sup> Adapted with permission from.<sup>6</sup> Copyright 2021 Springer Nature.

The dynamic range of electrochromic voltage sensing is closely linked to the FRET efficiency. To achieve higher sensitivity, the distance between the fluorescent donor and the retinal acceptor should be substantially reduced, which calls for the use of a small molecule fluorophore instead of a fluorescent protein. This could be achieved via PRIME method, which conjugates trans-cyclooctene (TCO) to a LAP peptide inserted into the first extracellular loop (ECL1) of an Ace2 mutant.<sup>18,19</sup> The enzymatic reaction proceeds via activation of the carboxylate into an adenylate intermediate, which then specifically reacts with the lysine side chain to form an amide linkage.<sup>20</sup> Thereafter, fluorophore labeling can be carried out using inverse electron demand Diels–Alder (IEDDA) reactions (Figure 1A).<sup>21–23</sup>

By introducing an alkyne-modified fluorescent dye via the CuAAC reaction, the resulting Flare1-Cy3 showed a sensitivity of  $-35.9\% \Delta F/F_0$  per 100 mV and was used to reveal gap junction-mediated electrical coupling in cultured human cells.<sup>24</sup> To address neural toxicity associated with CuAAC, the second-generation hybrid voltage indicator (HVI) adopted the more biocompatible IEDDA reaction (Figure 1B). HVI-Cy3 demonstrated improved sensitivity ( $-39.1\% \Delta F/F_0$  per 100 mV) and facilitate continuous recording of membrane voltage dynamics in neurons (Figure 1C).<sup>6</sup>

Further improvements in photostability and reduced phototoxicity were achieved by introducing a triplet state quencher cyclooctatetraene (COT) into the fluorophore structure. The resulting HVI-COT-Cy3 exhibited exceptional sensitivity ( $-52\% \Delta F/F_0$  per 100 mV) and substantially higher resistance to photobleaching, enabling continuous 30-min high-speed imaging in neurons. Additionally, the far-red indicator HVI-COT-Cy5 facilitated simultaneous dual-color imaging with the calcium indicator GCaMP6s for 15 min in neurons and cardiomyocytes.<sup>25</sup>

## BIOCONJUGATION VIA SELF-LABELING PROTEIN TAGS

Self-labeling protein tags have been pivotal in developing chemigenetic hybrid biosensors.<sup>11,12</sup> Among these, HaloTag is widely used in chemigenetic hybrid eFRET sensor development, due to its high labeling efficiency and the availability of HaloTag ligand-conjugated dyes, such as the Janelia Fluor dye series, which offer high fluorescence quantum yield and good biocompatibility (Figure 2A–C).<sup>26,27</sup> For example, when HaloTag was fused to the C-terminus of the Ace2 mutant and labeled with Janelia Fluor 525, the resulting sensor, Voltron<sub>525</sub>, exhibited a sensitivity of approximately  $-21\% \Delta F/F_0$  per 100 mV (Figure 2A). Due to the high photostability and molecular brightness of the Janelia Fluor dyes, Voltron records voltage signals with high signal-to-noise ratio in mouse, fruit fly, and zebrafish models.<sup>27</sup>

Further engineering of Ace2 rhodopsin has significantly enhanced its voltage-sensing properties. For instance, Ace2-(D81S)-HaloTag labeled with tetramethylrhodamine (TMR) showed approximately 45% improvement in AP sensitivity compared with Voltron<sub>525</sub>.<sup>28</sup> Additionally, Voltron<sub>2525</sub>, which includes an A122D mutation, demonstrated  $\sim 65\%$  greater sensitivity than Voltron<sub>525</sub> (approximately  $-35\% \Delta F/F_0$  per 100 mV). Voltron<sub>2525</sub> allows optical recording of multiple neurons in the mouse hippocampus (Figure 2D).<sup>29</sup> Mutations at the proton acceptor (D92) and release site (E199) of Ace2 transformed Voltron into Positron, a chemigenetic voltage sensor with a positive fluorescence-voltage response of approximately 19%  $\Delta F/F_0$  per 100 mV. Positron's lower molecular brightness in the resting state reduces background interference during larval zebrafish imaging.<sup>30</sup> Recently, Solaris, which utilizes the Ace2(D81S) mutant with a circularly permuted HaloTag (cpHaloTag) inserted into ECL1, achieved over a 2-fold increase in voltage sensitivity relative to Voltron<sub>525</sub> ( $-60.6\% \Delta F/F_0$  per 100 mV for Solaris<sub>525</sub>).<sup>19</sup>

Aside from microbial rhodopsin, the voltage-sensing domain (VSD), comprising four transmembrane helices (S1–S4) derived from voltage-sensing phosphatase, has also been utilized in constructing chemigenetic hybrid voltage indicators. In VSD-based indicators, voltage fluctuations induce conformational changes in the S4 helix, which is rich in positively charged residues. These conformational changes alter the chemical

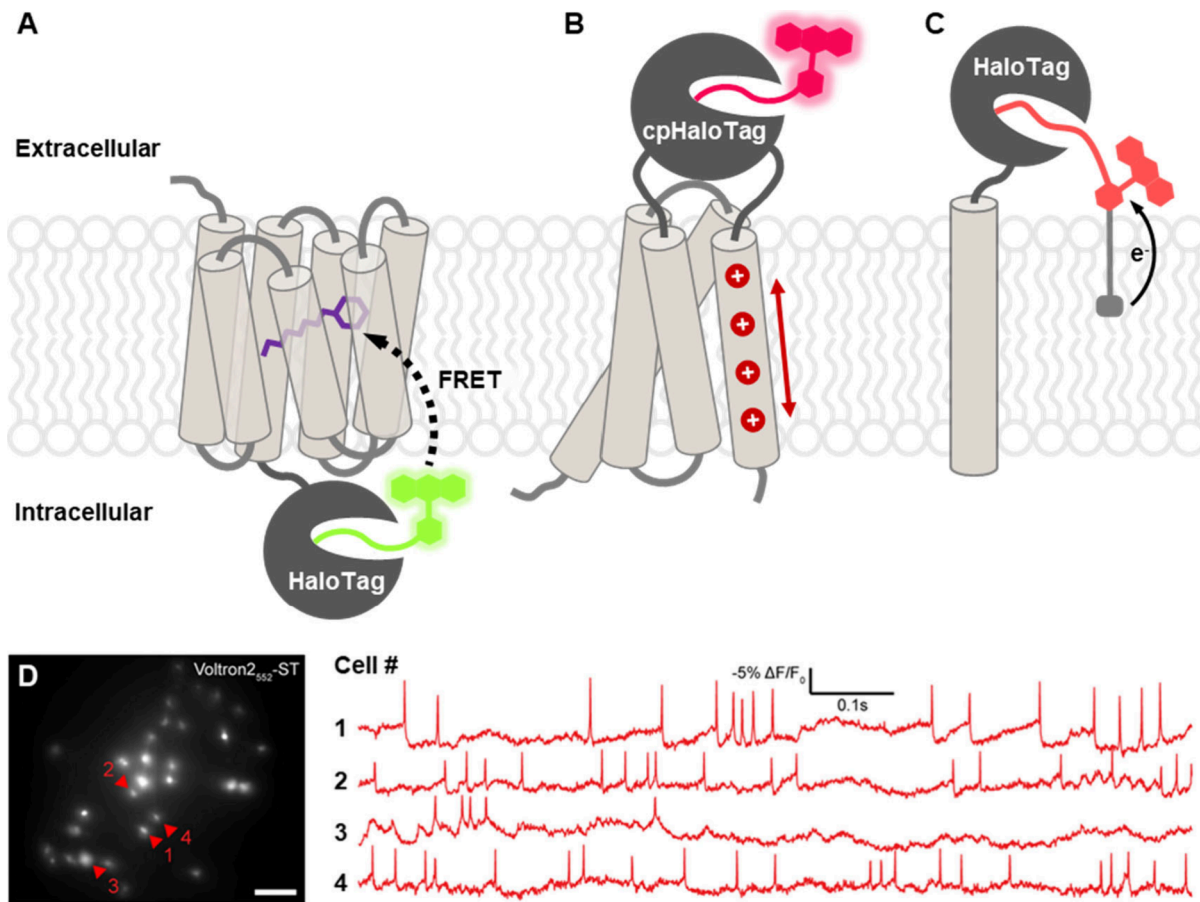


**Figure 2.** Chemigenetic voltage indicators enabled by self-labeling protein tags. (A) Scheme of self-labeling tag-assisted rhodopsin-based indicator (i.e., Voltron<sub>2525</sub><sup>29</sup>). (B) Scheme of self-labeling tag-assisted VSD-based indicator (i.e., HASAP<sub>635</sub><sup>34</sup>). (C) Scheme of self-labeling tag-targeted voltage-sensing dyes (i.e., RhoVR-Halo<sup>37</sup>). (D) Image of hippocampal PV neurons expressing Voltron<sub>2525</sub>-ST in mouse (left, scale bar = 200  $\mu$ m), and the fluorescence traces of 4 cells (right).<sup>29</sup> Adapted with permission from.<sup>29</sup> Copyright 2023 Elsevier.

**Table 1. Summary of Chemigenetic Hybrid Voltage Indicators**

Name	Sensor type	Conjugation method	Sensitivity $\Delta F/F_0$ (%)		Em. peak (nm)	Ext. coeff. $\epsilon$ ( $10^3$ M $^{-1}$ cm $^{-1}$ )	Quantum yield $\Phi$	Relative brightness <sup>b</sup>	ref.
			100 mV	AP <sup>a</sup>					
Flare1-Cy3	Rhodopsin	PRIME	-35.9	N.A.	569	150	0.10	0.45	24
HVI-Cy3	Rhodopsin	PRIME	-39.1	-25.3	574	150	0.10	0.45	6
HVI-Cy5	Rhodopsin	PRIME	-19.6	-12.8	667	271	0.28	2.26	6
HVI-COT-Cy3	Rhodopsin	PRIME	-52.0	-33.4	674	N.A.	N.A.	N.A.	25
HVI-COT-Cy5	Rhodopsin	PRIME	-16.0	-10.1	667	N.A.	N.A.	N.A.	25
Voltron <sub>525</sub>	Rhodopsin	HaloTag	-21	-6.2	553	84	0.87	2.17	27,29
Ace <sub>pRIS</sub> -HaloTag <sub>TMR</sub>	Rhodopsin	HaloTag	-19.1	-8.9	574	92	0.10	0.27	28
Voltron <sub>2525</sub>	Rhodopsin	HaloTag	-35	-10.1	553	84	0.87	2.17	29
Positron <sub>525</sub>	Rhodopsin	HaloTag	19	N.A.	553	84	0.87	2.17	30
Solaris <sub>585</sub>	Rhodopsin	HaloTag	-60.6	-28.1	611	109	0.83	2.70	19
VSD-HaloTag <sub>TMR</sub>	VSD	HaloTag	-2	N.A.	574	92	0.10	0.27	33
HArclight <sub>1635</sub>	VSD	HaloTag	-3.5	-3	656	81	0.75	1.81	34
HASAP <sub>1635</sub>	VSD	HaloTag	9.3	5	656	81	0.75	1.81	34
RhoVR-Halo	Organic dye	HaloTag	34	11.1	585	74	0.05	0.11	37
isoBeRST-Halo	Organic dye	HaloTag	21	10	677	N.A.	0.042	0.09	40

<sup>a</sup>Measured in cultured neurons <sup>b</sup>Calculated as the product of extinction coefficient and quantum yield of the fluorophore, normalized to the brightness of EGFP; N.A. not available.

environment of the attached fluorophore, leading to variations in fluorescence intensity.<sup>31,32</sup>

Initial attempts to use VSD from *Ciona intestinalis* (Ci-VSD) involved fusing HaloTag to its N- or C-terminus and labeling with TMR, resulting in a sensitivity of approximately  $-2\% \Delta F/$

$F_0$  per 100 mV.<sup>33</sup> Subsequently, the HArclight1<sub>635</sub> sensor adopted a similar *Ci*-VSD-HaloTag construct but used the Janelia Fluor 635 dye, which has a lactone-zwitterionic equilibrium more responsive to chemical environment changes. This resulted in a modest sensitivity of  $-3.5\% \Delta F/F_0$  per 100 mV.<sup>34</sup> Further advancements were made by incorporating a cpHaloTag into the extracellular loop of the S3 and S4 helices of the VSD from *Gallus gallus* (*Gg*-VSD). The resulting HASAP1<sub>635</sub> sensor exhibited significantly higher sensitivity, at 9.3%  $\Delta F/F_0$  per 100 mV (Figure 2B).<sup>34</sup>

Self-labeling tags offer not only a means to conjugate fluorescent ligands to voltage-sensing protein scaffolds but also serve as cell-specific markers for targeted labeling with ligand-modified organic voltage-sensitive dyes.<sup>35</sup> For example, when RhoVR (Rhodamine-based Voltage Reporters)<sup>36</sup> was conjugated with a HaloTag ligand, RhoVR-Halo was selectively bound to cell membranes displaying HaloTag (Figure 2C). This sensor exhibited a sensitivity of approximately 34%  $\Delta F/F_0$  per 100 mV through a photoinduced electron transfer (PeT) mechanism.<sup>37</sup> It was effectively used to detect excitatory postsynaptic potentials (EPSPs) in *Drosophila* neuromuscular junction and voltage fluctuations in brain explants,<sup>38</sup> and was demonstrated for two-photon (2P) imaging in mouse brain slices.<sup>37</sup> Similarly, the HaloTag ligand was conjugated to a silicon-rhodamine-based voltage-sensing dye with a far-red emission spectrum, known as BeRST1 (Berkeley Red Sensor of Transmembrane potential 1)<sup>39</sup>. The resulting isoBeRST-Halo showed a sensitivity of 21%  $\Delta F/F_0$  per 100 mV and was validated for specific labeling in cultured cells and mouse brain slices.<sup>40</sup>

## SUMMARY

In this Viewpoint, we provide a summary of the mechanisms, designs, properties, and applications of cutting-edge chemigenetic hybrid voltage indicators, which fall into two main categories based on bioconjugation chemistry: enzyme-mediated indicators and self-labeling tag-enabled indicators (Table 1). Overall, chemigenetic hybrid voltage indicators leverage the power of bioconjugation methods to combine the desirable properties of proteins (e.g., cell specificity) and small molecule fluorophores (e.g., high sensitivity, brightness, tunable emission spectra). Continued development of fast, specific, and *in vivo* compatible bioconjugation strategies will further enhance their utility in addressing biological questions.

## AUTHOR INFORMATION

### Corresponding Author

**Peng Zou** — College of Chemistry and Molecular Engineering, Synthetic and Functional Biomolecules Center, Beijing National Laboratory for Molecular Sciences, Key Laboratory of Bioorganic Chemistry and Molecular Engineering of Ministry of Education and PKU-IDG/McGovern Institute for Brain Research, Peking-Tsinghua Center for Life Sciences, Peking University, Beijing 100871, China; Chinese Institute for Brain Research (CIBR), Beijing 102206, China;  orcid.org/0000-0002-9798-5242; Email: [zoupeng@pku.edu.cn](mailto:zoupeng@pku.edu.cn)

### Author

**Shuzhang Liu** — College of Chemistry and Molecular Engineering, Synthetic and Functional Biomolecules Center, Beijing National Laboratory for Molecular Sciences, Key Laboratory of Bioorganic Chemistry and Molecular

Engineering of Ministry of Education, Peking University, Beijing 100871, China

Complete contact information is available at:  
<https://pubs.acs.org/10.1021/acs.bioconjchem.4c00383>

### Author Contributions

P.Z. conceptualized the Viewpoint article; S.L. wrote the draft; S.L. and P.Z. edited the manuscript.

### Notes

The authors declare no competing financial interest.

## ACKNOWLEDGMENTS

This work was supported by the Ministry of Science and Technology (2022YFA1304700), the National Natural Science Foundation of China (32088101), and Beijing National Laboratory for Molecular Sciences (BNLMS-CXXM-202403). P.Z. is sponsored by Bayer Investigator Award.

## REFERENCES

- (1) Cohen, A. E.; Venkatachalam, V. Bringing bioelectricity to light. *Annu Rev Biophys* **2014**, *43*, 211–232.
- (2) Levin, M. Molecular bioelectricity: How endogenous voltage potentials control cell behavior and instruct pattern regulation *in vivo*. *Mol. Biol. Cell* **2014**, *25*, 3835–3850.
- (3) Huang, C. L. H.; Lei, M. Cardiomyocyte electrophysiology and its modulation: Current views and future prospects. *Philos T R Soc B* **2023**, *378*, No. 20220160.
- (4) Rorsman, P.; Ashcroft, F. M. Pancreatic  $\beta$ -cell electrical activity and insulin secretion: Of mice and men. *Physiol Rev* **2018**, *98*, 117–214.
- (5) Kulkarni, R. U.; Miller, E. W. Voltage imaging: Pitfalls and potential. *Biochemistry* **2017**, *56*, 5171–5177.
- (6) Liu, S. Z.; Lin, C.; Xu, Y. X.; Luo, H. X.; Peng, L. X.; Zeng, X. M.; Zheng, H. T.; Chen, P. R.; Zou, P. A far-red hybrid voltage indicator enabled by bioorthogonal engineering of rhodopsin on live neurons. *Nat Chem* **2021**, *13*, 472–479.
- (7) Fernández-Suárez, M.; Baruah, H.; Martínez-Hernández, L.; Xie, K. T.; Baskin, J. M.; Bertozzi, C. R.; Ting, A. Y. Redirecting lipoic acid ligase for cell surface protein labeling with small-molecule probes. *Nat. Biotechnol.* **2007**, *25*, 1483–1487.
- (8) Putthenveetil, S.; Liu, D. S.; White, K. A.; Thompson, S.; Ting, A. Y. Yeast display evolution of a kinetically efficient 13-amino acid substrate for lipoic acid ligase. *J. Am. Chem. Soc.* **2009**, *131*, 16430–16438.
- (9) Gautier, A.; Juillerat, A.; Heinis, C.; Correa, I. R., Jr.; Kindermann, M.; Beaufils, F.; Johnsson, K. An engineered protein tag for multiprotein labeling in living cells. *Chem Biol* **2008**, *15*, 128–136.
- (10) Los, G. V.; Encell, L. P.; McDougall, M. G.; Hartzell, D. D.; Karassina, N.; Zimprich, C.; Wood, M. G.; Learish, R.; Ohana, R. F.; Urh, M.; et al. HaloTag: A novel protein labeling technology for cell imaging and protein analysis. *ACS Chem Biol* **2008**, *3*, 373–382.
- (11) Wang, A. Q.; Feng, J. S.; Li, Y. L.; Zou, P. Beyond fluorescent proteins: Hybrid and bioluminescent indicators for imaging neural activities. *ACS Chem Neurosci* **2018**, *9*, 639–650.
- (12) Liu, S. Z.; Yang, J. Q.; Zou, P. Bringing together the best of chemistry and biology: Hybrid indicators for imaging neuronal membrane potential. *J Neurosci Meth* **2021**, *363*, No. 109348.
- (13) Kralj, J. M.; Douglass, A. D.; Hochbaum, D. R.; Maclaurin, D.; Cohen, A. E. Optical recording of action potentials in mammalian neurons using a microbial rhodopsin. *Nat Methods* **2012**, *9*, 90–95.
- (14) Maclaurin, D.; Venkatachalam, V.; Lee, H.; Cohen, A. E. Mechanism of voltage-sensitive fluorescence in a microbial rhodopsin. *Proc Natl Acad Sci USA* **2013**, *110*, 5939–5944.
- (15) Gong, Y. Y.; Huang, C.; Li, J. Z.; Grewe, B. F.; Zhang, Y. P.; Eismann, S.; Schnitzer, M. J. High-speed recording of neural spikes in awake mice and flies with a fluorescent voltage sensor. *Science* **2015**, *350*, 1361–1366.

- (16) Zou, P.; Zhao, Y. X.; Douglass, A. D.; Hochbaum, D. R.; Brinks, D.; Werley, C. A.; Harrison, D. J.; Campbell, R. E.; Cohen, A. E. Bright and fast multicoloured voltage reporters via electrochromic FRET. *Nat Commun* **2014**, *5*, 4625.
- (17) Gong, Y. Y.; Wagner, M. J.; Li, J. Z.; Schnitzer, M. J. Imaging neural spiking in brain tissue using FRET-opsin protein voltage sensors. *Nat Commun* **2014**, *5*, 3674.
- (18) Han, Y.; Yang, J.; Li, Y.; Chen, Y.; Ren, H.; Ding, R.; Qian, W.; Ren, K.; Xie, B.; Deng, M.; et al. Bright and sensitive red voltage indicators for imaging action potentials in brain slices and pancreatic islets. *Sci Adv* **2023**, *9*, 4208.
- (19) Yang, J.; Zhu, S.; Yang, L.; Peng, L.; Han, Y.; Hayward, R. F.; Park, P.; Hu, D.; Cohen, A. E.; Zou, P. Solaris: A panel of bright and sensitive hybrid voltage indicators for imaging membrane potential in cultured neurons. *bioRxiv*, Feb. 4, 2024. DOI: 10.1101/2024.02.02.578569
- (20) Liu, D. S.; Nivón, L. G.; Richter, F.; Goldman, P. J.; Deerinck, T. J.; Yao, J. Z.; Richardson, D.; Phipps, W. S.; Ye, A. Z.; Ellisman, M. H.; et al. Computational design of a red fluorophore ligase for site-specific protein labeling in living cells. *Proc Natl Acad Sci USA* **2014**, *111*, 4551–4559.
- (21) Uttamapinant, C.; Tangpeerachaikul, A.; Grecian, S.; Clarke, S.; Singh, U.; Slade, P.; Gee, K. R.; Ting, A. Y. Fast, cell-compatible click chemistry with copper-chelating azides for biomolecular labeling. *Angew Chem Int Edit* **2012**, *51*, 5852–5856.
- (22) Yao, J. Z.; Uttamapinant, C.; Poloukhtine, A.; Baskin, J. M.; Codelli, J. A.; Sletten, E. M.; Bertozzi, C. R.; Popik, V. V.; Ting, A. Y. Fluorophore targeting to cellular proteins via enzyme-mediated azide ligation and strain-promoted cycloaddition. *J. Am. Chem. Soc.* **2012**, *134*, 3720–3728.
- (23) Liu, D. S.; Tangpeerachaikul, A.; Selvaraj, R.; Taylor, M. T.; Fox, J. M.; Ting, A. Y. Diels-Alder cycloaddition for fluorophore targeting to specific proteins inside living cells. *J. Am. Chem. Soc.* **2012**, *134*, 792–795.
- (24) Xu, Y. X.; Peng, L. X.; Wang, S. C.; Wang, A. Q.; Ma, R. R.; Zhou, Y.; Yang, J. H.; Sun, D. E.; Lin, W.; Chen, X.; et al. Hybrid indicators for fast and sensitive voltage imaging. *Angew Chem Int Edit* **2018**, *57*, 3949–3953.
- (25) Liu, S. Z.; Ling, J.; Chen, P.; Cao, C.; Peng, L. X.; Zhang, Y.; Ji, G. S.; Guo, Y. N.; Chen, P. R.; Zou, P.; et al. Orange/far-red hybrid voltage indicators with reduced phototoxicity enable reliable long-term imaging in neurons and cardiomyocytes. *Proc Natl Acad Sci USA* **2023**, *120*, No. e2306950120.
- (26) Grimm, J. B.; Muthusamy, A. K.; Liang, Y. J.; Brown, T. A.; Lemon, W. C.; Patel, R.; Lu, R. W.; Macklin, J. J.; Keller, P. J.; Ji, N.; et al. A general method to fine-tune fluorophores for live-cell and imaging. *Nat Methods* **2017**, *14*, 987.
- (27) Abdelfattah, A. S.; Kawashima, T.; Singh, A.; Novak, O.; Liu, H.; Shuai, Y. C.; Huang, Y. C.; Campagnola, L.; Seeman, S. C.; Yu, J. N.; et al. Bright and photostable chemogenetic indicators for extended in vivo voltage imaging. *Science* **2019**, *365*, 699.
- (28) Xu, Y. X.; Deng, M. Y.; Zhang, S.; Yang, J. Q.; Peng, L. X.; Chu, J.; Zou, P. Imaging neuronal activity with fast and sensitive red-shifted electrochromic FRET indicators. *ACS Chem Neurosci* **2019**, *10*, 4768–4775.
- (29) Abdelfattah, A. S.; Zheng, J. H.; Singh, A.; Huang, Y. C.; Reep, D.; Tsegaye, G.; Tsang, A.; Arthur, B. J.; Rehorova, M.; Olson, C. V. L.; et al. Sensitivity optimization of a rhodopsin-based fluorescent voltage indicator. *Neuron* **2023**, *111*, 1547.
- (30) Abdelfattah, A. S.; Valenti, R.; Zheng, J.; Wong, A.; Chuong, A. S.; Hasseman, J. P.; Jayaraman, V.; Kolb, I.; Korff, W.; Lavis, L. D.; et al. A general approach to engineer positive-going eFRET voltage indicators. *Nat Commun* **2020**, *11*, 3444.
- (31) Jin, L.; Han, Z.; Platasa, J.; Wooltorton, J. R. A.; Cohen, L. B.; Pieribone, V. A. Single action potentials and subthreshold electrical events imaged in neurons with a fluorescent protein voltage probe. *Neuron* **2012**, *75*, 779–785.
- (32) St-Pierre, F.; Marshall, J. D.; Yang, Y.; Gong, Y. Y.; Schnitzer, M. J.; Lin, M. Z. High-fidelity optical reporting of neuronal electrical activity with an ultrafast fluorescent voltage sensor. *Nat Neurosci* **2014**, *17*, 884–889.
- (33) Tsutsui, H.; Jinno, Y.; Tomita, A.; Okamura, Y. Optically detected structural change in the N-terminal region of the voltage-sensor domain. *Biophys. J.* **2013**, *105*, 108–115.
- (34) Deo, C.; Abdelfattah, A. S.; Bhargava, H. K.; Berro, A. J.; Falco, N.; Farrants, H.; Moeyaert, B.; Chupanova, M.; Lavis, L. D.; Schreiter, E. R. The HaloTag as a general scaffold for far-red tunable chemogenetic indicators. *Nat Chem Biol* **2021**, *17*, 718–723.
- (35) Liu, P.; Miller, E. W. Electrophysiology, unplugged: Imaging membrane potential with fluorescent indicators. *Acc. Chem. Res.* **2020**, *S3*, 11–19.
- (36) Deal, P. E.; Kulkarni, R. U.; Al-Abdullatif, S. H.; Miller, E. W. Isomerically pure tetramethylrhodamine voltage reporters. *J. Am. Chem. Soc.* **2016**, *138*, 9085–9088.
- (37) Deal, P. E.; Liu, P.; Al-Abdullatif, S. H.; Muller, V. R.; Shamardani, K.; Adesnik, H.; Miller, E. W. Covalently tethered rhodamine voltage reporters for high speed functional imaging in brain tissue. *J. Am. Chem. Soc.* **2020**, *142*, 614–622.
- (38) Kirk, M. J.; Benlian, B. R.; Han, Y. F.; Gold, A.; Ravi, A.; Deal, P. E.; Molina, R. S.; Drobizhev, M.; Dickman, D.; Scott, K.; et al. Voltage imaging in drosophila using a hybrid chemical-genetic rhodamine voltage reporter. *Front Neurosci* **2021**, *15*, No. 754027.
- (39) Huang, Y. L.; Walker, A. S.; Miller, E. W. A photostable silicon rhodamine platform for optical voltage sensing. *J. Am. Chem. Soc.* **2015**, *137*, 10767–10776.
- (40) Ortiz, G.; Liu, P.; Deal, P. E.; Nensel, A. K.; Martinez, K. N.; Shamardani, K.; Adesnik, H.; Miller, E. W. A silicon-rhodamine chemical-genetic hybrid for far red voltage imaging from defined neurons in brain slice. *RSC Chem Biol* **2021**, *2*, 1594–1599.